High-Temperature Kinetics of Si-Containing Precursors for Ceramic Processing

D. Woiki, L. Catoire, and P. Roth
Institut für Verbrennung und Gasdynamik, Gerhard-Mercator-Universität Duisburg, 47048 Duisburg, Germany

Experimental investigations of high-temperature kinetics of Si-precursor molecules relevant to CVD and ceramic processing are described. Reaction systems using SiH_4, Si_2H_6, and $SiCl_4$ highly diluted in argon were studied in a shock tube, a high-temperature wave reactor, by monitoring in situ the concentrations of atomic or radical reactants Si, H, Cl, SiH, and SiH_2. Because of the very high dilution, the measured properties are sensitive to a limited number of elementary reactions, allowing a relatively direct determination of the respective rate coefficients. Both thermal pyrolysis and laser flash photolysis methods were used to expand the investigated temperature range. An overview of the bimolecular Si-atom reactions is given.

Introduction

Chemical processes of silicon-containing gases are of great interest because of their major role in chemical vapor deposition (CVD) techniques for semiconductor manufacturing as well as in the production of new ceramic materials. Detailed modeling of the fluid dynamics and gas-phase chemistry is desirable for both controlling and optimizing of processes, and might also lead to novel apparatus design. Coltrin et al. (1986) have developed a numerical model for simulations of silane CVD reactors, which has also been used for simulations of measured species concentrations; see, for example, Breiland et al. (1986). A key prediction of this model is that considerable chemistry occurs in the gas phase and that, under certain conditions, gas-phase intermediates contribute to deposition. Predictive simulations of CVD systems require, among other things, a complete set of both thermodynamic data for all relevant species and accurate kinetic data for elementary reactions. However, the availability of these data, especially at elevated temperatures, is very limited.

We intend to give an overview of recent high-temperature shock-tube investigations on silane reaction systems in our laboratory. The large number of reactions and systems considered here prevent a detailed compilation of the earlier experimental work. This and also details of RRKM calculations for the pyrolysis reactions can be found in the references.

The combination of a shock tube with laser photolysis and sensitive, quantitative absorption diagnostics presents a powerful tool for investigating the reaction kinetics of Si-containing systems. Shock tubes are high-temperature wave reactors, in which homogeneous reactions can be studied under diffusion-free conditions. These reactions can be initiated either by the steplike temperature increase of the bath gas or, at somewhat lower temperatures, by the photodissociation of precursor molecules providing free radicals as reaction educts. The two sensitive absorption diagnostics applied, atomic resonance absorption spectroscopy (ARAS) and ring-dye-laser absorption spectroscopy (RDLAS), allow time-resolved concentration measurements of atoms and free radicals in the sub-ppm concentration range. Therefore, the reaction systems can be designed with very high inert-gas dilution, which can provide quasiisolation of a few key elementary reactions and thus strongly facilitate the interpretation of the experiments. The studies presented here are typical for the powerful way in which those methods of shock tubes can be used to investigate high-temperature chemical kinetic problems.

Experimental Studies

The experiments were carried out behind reflected shock waves in two different shock tubes, both made of stainless steel and specially prepared for ultra-high-vacuum (UHV) purposes. Both tubes have similar dimensions with an internal diameter of 79 mm or 80 mm and driven sections of 5.7 m or 6.0 m in length. They can be baked out and pumped down to pressures below 5×10^{-8} mbar by turbo molecular pumps. Gas mixtures were prepared manometrically in stainless-steel UHV storage cylinders by using calibrated pressure gauges. Only gases of the highest commerically available purity were

Correspondence concerning this article should be addressed to P. Roth
L. Catoire is on leave from LCSR, CNRS, Orleans, France.

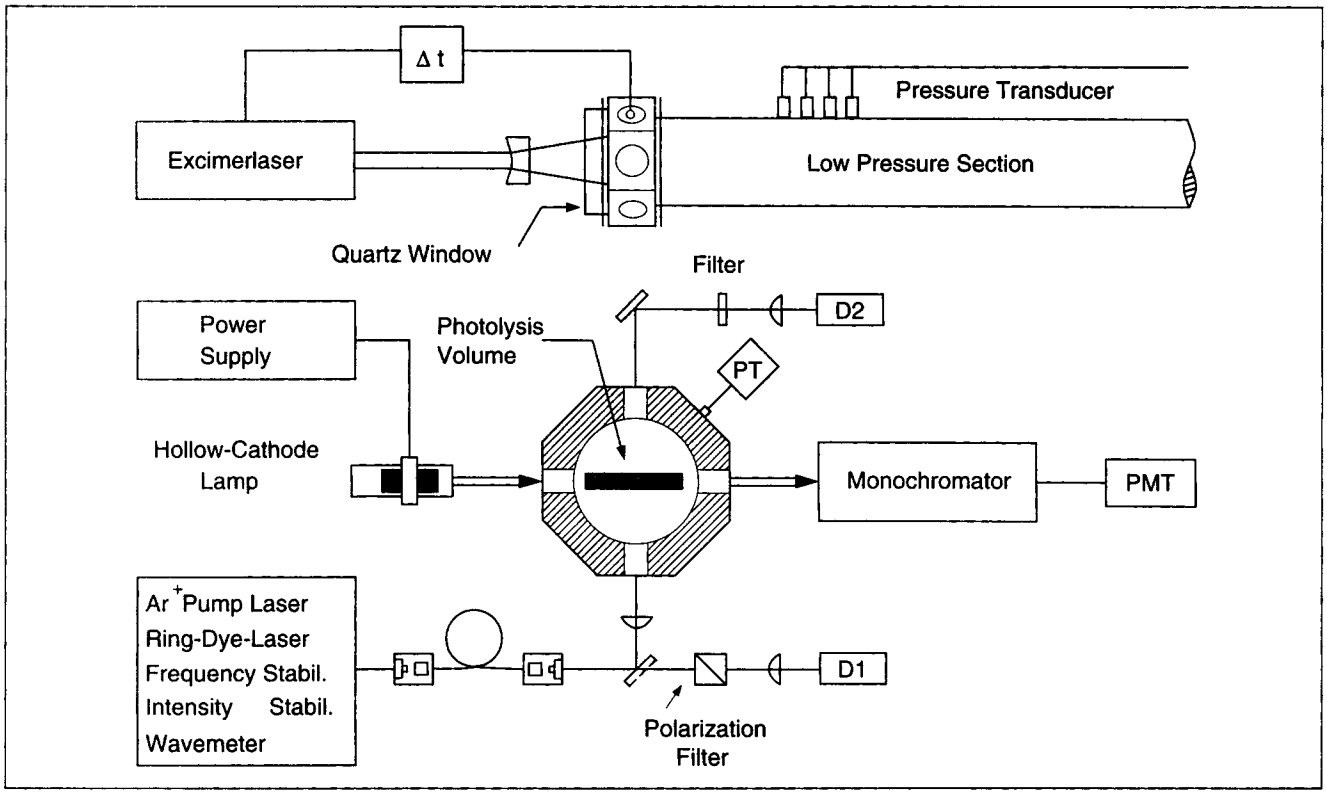

Figure 1. Experimental measurements in a shock tube.

Atomic resonance absorption spectroscopy (ARAS), ring-dye-laser spectroscopy (RDLS), and laser flash photolysis (LFP).

used. $SiCl_4$, which is a liquid at normal conditions, was evaporated in a separate evaporation vessel. The residual gases in all UHV devices were analyzed by quadrupole mass spectrometers, and were found to be practically free of hydrocarbons. One of the shock tubes shown in Figure 1 is equipped with an excimer laser for laser flash photolysis (LFP) experiments. The laser light ($\lambda = 193$ nm) of a Lambda Physik type EMC 150 T MSC ArF-excimer laser was coupled into the measurement plane of this shock tube through an end plate made of quartz glass. The rectangular laser beam was expanded by a cylindrical lens, allowing the illumination of the whole diagnostic pathway. The laser was operated in single-pulse mode. It had a pulse width of 13 ns and an average energy of 55 mJ $\pm$ 7 mJ per pulse, measured behind the quartz-glass window of the shock tube. A detailed description of the apparatus and the experimental procedure is given in Thielen and Roth (1987), Woiki et al. (1993), and Woiki and Roth (1994).

Si-, H-, Cl-atom concentrations were measured using ARAS. The optical arrangement consists of a pulsed hollow-cathode lamp for Si-atoms (configuration shown in Figure 1) or a microwave discharge lamp for H- and Cl-atoms, the absorption path in the shock tube, a monochromator, and a photomultiplier. The relation between the measured absorption A_X and the corresponding species concentration is given by the modified Lambert-Beer law:

$$A_X = 1 - \exp\left[-(l \times \sigma_X/\mathrm{cm}^3) \times ([X]/\mathrm{cm}^{-3})^n\right]; \quad X = \mathrm{Si, H, Cl}, \quad (1)$$

where the concentration exponent n was introduced to improve the description of the nonideal line-emission/line-absorption of ARAS. For ARAS measurements calibration is necessary due to the unknown spectral line shape emitted from the lamp. The atomic absorption cross sections were determined in a series of calibration experiments with known concentrations for Si-, H-, and Cl-atoms from the very rapid dissociation of SiH_4, $SiCl_4$, $TiCl_4$ or H_2 at high temperatures (see Table 1).

SiH and SiH_2 were measured by RDLAS. SiH_2 measurements were made using the Q-branch of the $\tilde{A}-\tilde{X}(0,2,0)-(0,0,0)$ band near 579.35 nm, and SiH measurements were made using the Q-branch of the $\tilde{A}-\tilde{X}(0,0)$ band near 413.5 nm. Monochromatic radiation was generated using a conventional ring dye laser, stabilized in both frequency

Table 1. Wavelength and Absorption Cross Sections or Absorption Coefficients for Absorption Measurements of the Present Study*

Species X	Wavelength nm	σ_x cm^2	n
Si	251.6	5.5×10^{-11}	0.8
H	121.6	1.1×10^{-11}	0.8
Cl	134.7	7.5×10^{-14}	0.8
Species Y		$\alpha_{v,Y}/(\mathrm{cm}^{-1}\cdot\mathrm{bar}^{-1})$	
SiH_2	579.35	5.4×10^{1}	
SiH	413.53	1.3×10^{3}	

*Reference conditions for SiH_2-RDLAS: $T = 1{,}700$ K and $p = 0.3$ bar; SiH-RDLAS: $T = 1{,}700$ K and $p = 1.0$ bar.

and intensity and pumped by a CW-Ar^+ laser. The laser light was introduced into the measurement plane of the shock tube using an optical fiber, and the intensities of probe beam and reference beam were detected with silicon photo diodes. The relation between measured absorption and the corresponding radical partial pressure p_Y is again given by the Lambert-Beer law:

$$A_Y = 1 - \exp[-(l \times \alpha_{\upsilon,Y})/\mathrm{bar}^{-1} \times p_Y/\mathrm{bar}]; \qquad Y = \mathrm{SiH}, \mathrm{SiH_2}. \quad (2)$$

In the present case of narrow-bandwidth laser absorption, the absorption coefficient α_υ of a single line transition is proportional to the Boltzmann fraction of the population of the lower transition level $f_B(T)$, the line strength for the given rotational transition $f_{J'J''}$, and the line-shape factor $\Phi(T,p,\upsilon)$, which describes the influence of line-broadening processes

$$\alpha_\upsilon(p,T,\upsilon) = \mathrm{const.} \times f_B(T) \times f_{J'J''} \times \Phi(T,P,\upsilon). \quad (3)$$

The line strength $f_{J'J''}$ and the collisional line broadening, which has influence on the shape factor $\Phi(T,p,\upsilon)$, were determined in separate shock-wave experiments (see Markus and Roth, 1994, 1996). A reference value for the absorption coefficient of SiH_2 was obtained from Si_2H_6 shock-tube experiments at conditions, for which an *a priori* calculation of the SiH_2 concentration was possible within error limits of ±15%. For SiH radicals a calculation of the absorption cross section was possible after determining the line-shape factor $\Phi(T,p,\upsilon)$ using a characteristic line shape, which strongly depends on pressure of a partly resolved Λ-type doublet. The temperature and pressure dependence of the absorption coefficient was calculated based on a spectroscopic model (see Markus and Roth, 1994, 1996). A summary of the absorption cross sections for ARAS and of the absorption coefficients for RDLAS regarded in the present study is given in Table 1, where the values for SiH_2 and SiH are valid for the given reference conditions.

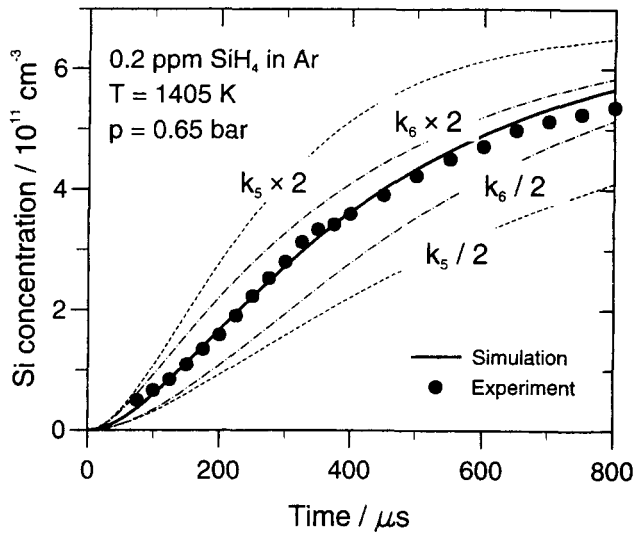

Figure 2. Measured (points) vs. calculated Si concentration profiles in an SiH_4/Ar pyrolysis experiment.

Simulation is based on the reaction mechanism of Table 2. Variations of k_5 and k_6 are shown as thin lines.

Results

Pyrolysis of silane

The pyrolysis of silane was studied in the temperature range between 1250 and 1715 K at pressures between 0.6 and 0.8 bar with initial mixtures between 0.15 and 1.5 ppm SiH_4 diluted in Ar by monitoring the resonance absorption of Si atoms. The measured absorption signals were transferred into concentration profiles by applying the calibration described earlier. A typical Si-atom concentration profile observed in a reaction system with 0.2 ppm SiH_4 is shown in Figure 2; see dots. This and all other profiles were evaluated by computer simulations based on the reaction mechanism of Table 2 by varying the rate coefficients k_5 and k_6 of the decomposition reactions:

Table 2. Simplified Reaction Mechanism for Highly Diluted SiH_4 and Si_2H_6 Pyrolysis and Photolysis Experiments*

No.			Reaction			Rate Coefficient A	Rate Coefficient T_a
R1	Si_3H_8		$\rightleftharpoons SiH_2$	$+Si_2H_6$		7.8×10^{14}	25,630
R2	Si_3H_8		$\rightleftharpoons H_3SiSiH$	$+SiH_4$		5.5×10^{15}	26,190
R3	Si_2H_6		$\rightleftharpoons SiH_4$	$+SiH_2$		5.2×10^{10}	16,850
R4	Si_2H	+M	$\rightarrow Si_2$	+H	+M	3.0×10^{15}	20,000
R5	SiH_4		$\rightleftharpoons SiH_2$	$+H_2$		1.9×10^{10}	22,550
R6	SiH_2	+M	$\rightleftharpoons Si$	$+H_2$	+M	9.1×10^{13}	15,100
R7	H_2	+M	$\rightleftharpoons H$	+H	+M	2.2×10^{14}	48,300
R8	SiH_4	$+SiH_2$	$\rightleftharpoons H_3SiSiH$	$+H_2$		1.3×10^{13}	0
R9	SiH_2	+Si	$\rightarrow Si_2H$	+H		5.0×10^{14}	0
R10	SiH_2	$+SiH_2$	$\rightleftharpoons Si_2H_2$	$+H_2$		6.5×10^{14}	0
R11	SiH	$+H_2$	$\rightleftharpoons SiH_2$	+H		4.8×10^{14}	11,900
R12	SiH	$+SiH_4$	$\rightleftharpoons Si_2H_4$	+H		1.6×10^{14}	0
R13	Si	$+H_2$	$\rightleftharpoons SiH$	+H		1.5×10^{15}	16,000
R14	Si	$+SiH_4$	$\rightleftharpoons Si_2H_2$	$+H_2$		4.0×10^{14}	0
R15	Si	$+Si_2H_6$	$\rightleftharpoons Si_3H_2$	$+2H_2$		4.8×10^{14}	0
R16	H_3SiSiH		$\rightleftharpoons H_2SiSiH_2$			7.9×10^{12}	5,300

*The compilation of the rate coefficients $k_j = A_j \times \exp(-T_{a,j}/T)$ $\mathrm{cm^3 \cdot mol^{-1} \cdot s^{-1}}$ or $\mathrm{s^{-1}}$ is described by Mick et al. (1993a, 1995a).

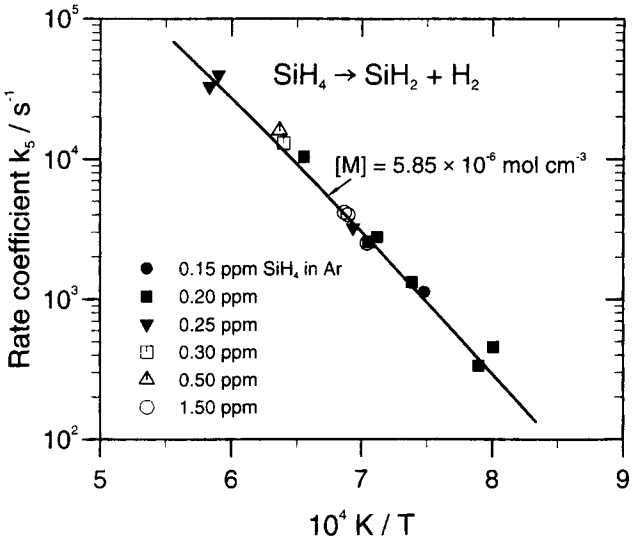

Figure 3. Arrhenius diagram of the dissociation rate coefficient k_5.

It includes results obtained from experiments (points) and from RRKM calculations of Mick et al. (1993a).

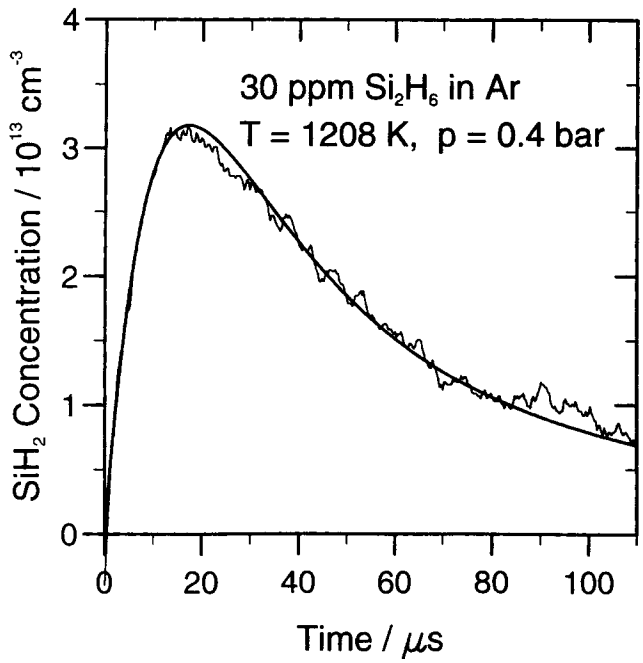

Figure 4. Measured vs. calculated SiH_2 concentration profiles in an Si_2H_6/Ar prolysis experiment.

Simulation is based on the reaction mechanism of Table 2.

$$SiH_4 \overset{k_5}{\rightleftharpoons} SiH_2 + H_2 \qquad \Delta h^R = 237 \text{ kJ/mol} \qquad (R5)$$

$$SiH_2 + M \overset{k_6}{\rightleftharpoons} Si + H_2 + M \qquad \Delta h^R = 382 \text{ kJ/mol.} \qquad (R6)$$

An individual result of this fitting is shown in Figure 2. The additional lines in Figure 2 illustrate the sensitivity with respect to variations of the two rate coefficients. The data points for the rate coefficient k_5 are plotted in the Arrhenius diagram of Figure 3, and can be expressed for the concentration range of the experiments of $4.7\times10^{-6} \le [M]/\text{mol cm}^{-3} \le 7.0 \times10^{-6}$, which is in the fall-off range, by:

$$k_5 = 1.9\times10^{10}\exp(-22{,}500\ \text{K}/T)\text{s}^{-1}.$$

A discussion of the pressure dependence of k_5 based on RRKM calculations is given by Mick et al. (1993a).

Pyrolysis of disilane

The pyrolysis of disilane was studied in the temperature range between 1,070 and 1,380 K at pressures between 0.35 and 1.28 bar with initial mixtures between 15 and 50 ppm Si_2H_6 diluted in Ar by measuring SiH_2 concentration profiles. A typical example is illustrated in Figure 4. After the reflected-shock arrival ($t = 0$), the SiH_2 radicals were generated very rapidly within the first 20 μs and decrease close to zero during the following time interval of about 100 μs. Additional Si-atom measurements in higher diluted systems with 0.1 to 0.25 ppm Si_2H_6 showed a Si-conversion yield of $[Si]_{max}/(2\times[Si_2H_6]_0 \approx 1$. Both, the Si-atom and the SiH_2-radical concentration profiles could be simulated by the simplified reaction mechanism of Table 2. By comparing measured Si-concentration profiles with computer simulations the reaction,

$$Si_2H_6 \overset{k_3}{\rightleftharpoons} SiH_4 + SiH_2 \qquad \Delta h^R = 222 \text{ kJ/mol,} \qquad (R3)$$

was identified as the initial decomposition step. The rate coefficient k_3 was determined from fittings of calculated SiH_2 profiles to measured ones (see Figure 4). All k_3-values obtained are summarized in the Arrhenius diagram of Figure 5. RRKM calculation described by Mick et al. (1995a) was used for further data interpretation. As a result of these calcula-

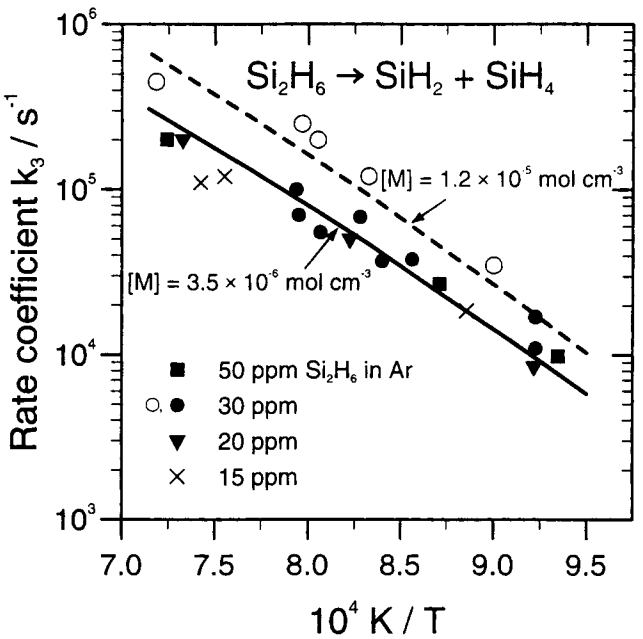

Figure 5. Arrhenius diagram of the dissociation rate coefficient k_3.

It includes the results obtained from experiments (points) and from RRKM calculations of Mick et al. (1995a).

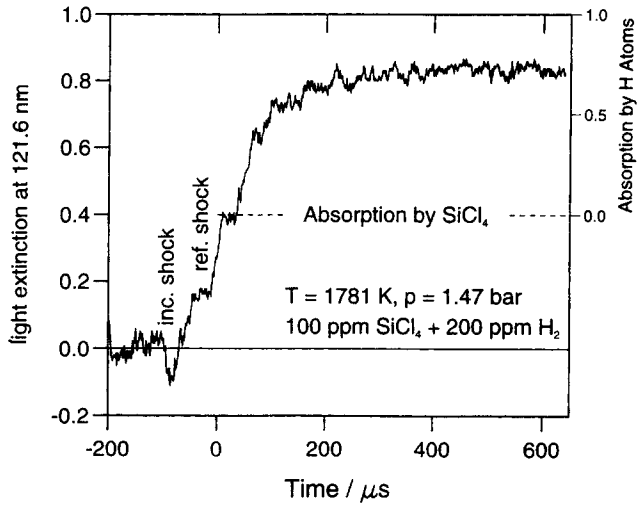

Figure 6. Typical example of L_α absorption observed in an $SiCl_4/H_2/Ar$ pyrolysis experiment.

The signal is composed of two parts: a constant absorption of $SiCl_4$ and a time-dependent absorption of H atoms.

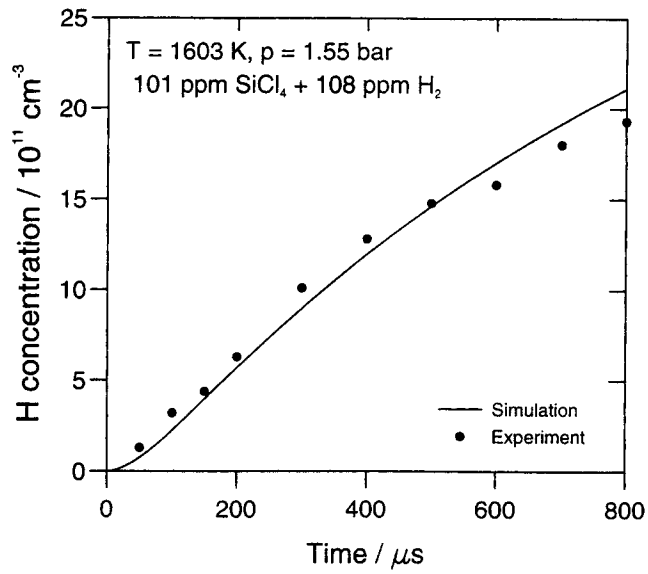

Figure 7. Measured (points) and calculated (line) concentration profiles of H atoms in a pyrolysis experiment with $SiCl_4/H_2/Ar$ gas mixture.

Simulation is based on the reaction mechanism of Table 3.

tions, the two lines in Figure 5 illustrate mean values of k_3 for two different absolute concentrations [M].

Pyrolysis of silicon tetrachloride

The pyrolysis of silicon tetrachloride was studied at temperatures between 1,550 and 1,670 K and pressures between 1.0 and 1.5 bar by using H-atom ARAS in $SiCl_4/H_2/Ar$ systems. At temperatures between 2,070 and 2,370 K and pressures of about 1.5-bar, molecular absorption of $SiCl_4$ at 121.6 nm in the $SiCl_4/Ar$ systems was additionally used to follow the decay of $SiCl_4$. A typical H-atom absorption signal obtained from a mixture of 100 ppm $SiCl_4$ + 200 ppm H_2 diluted in Ar at $T = 1{,}780$ K is shown in Figure 6. All the experimental profiles were analyzed by a fitting procedure based on the reaction mechanism of Table 3. The first decomposition step, the elimination of Cl, is favored over the elimination of Cl_2 by kinetic and energetic considerations.

$$SiCl_4 + M \overset{k_{17}}{\rightleftharpoons} SiCl_3 + Cl + M \qquad \Delta h^R = 466 \text{ kJ/mol.} \quad \text{(R17)}$$

Table 3. Simplified Reaction Mechanism Established to Verify the Observed Si-, Cl- and H-atom Formation in $SiCl_4/Ar$ (R17 to R22) and $SiCl_4/H_2/Ar$ (R17, R21 to R25) Systems*

No.	Reaction				Rate Coefficient A	n	T_a
R17	$SiCl_4$	$+M \rightleftharpoons SiCl_3$	$+Cl$	$+M$	4.8×10^{16}	0	40,954
R18	$SiCl_3$	$+M \rightleftharpoons SiCl_2$	$+Cl$	$+M$	3.7×10^{14}	0	31,730
R19	$SiCl_2$	$+M \rightleftharpoons SiCl$	$+Cl$	$+M$	9.4×10^{14}	0	43,250
R20	$SiCl$	$+M \rightleftharpoons Si$	$+Cl$	$+M$	9.3×10^{14}	0	39,190
R21	Cl_2	$-M \rightleftharpoons Cl$	$+Cl$	$+M$	2.3×10^{13}	0	23,632
R22	$Si+Si$	$+M \rightleftharpoons Si_2$	$+$	$+M$	2.5×10^{16}	0	594
R23	$SiCl_4$	$+H \rightleftharpoons SiCl_3$	$+HCl$		1.4×10^{13}	0	4,800
R24	HCl	$+M \rightleftharpoons H$	$+Cl$	$+M$	4.4×10^{13}	0	41,144
R7	H_2	$+M \rightleftharpoons H$	$+H$	$+M$	2.2×10^{14}	0	48,355
R25	H_2	$+Cl \rightleftharpoons H$	$+HCl$		1.4×10^{8}	1.63	1,592

*The compilation of the rate coefficients $k_j = A_j \times T^n \times \exp(-T_{a,j}/T)$ $cm^3 \cdot mol^{-1} \cdot s^{-1}$ is described by Catoire et al. (1997a,b).

A typical example of a measured H-concentration profile compared with a computer simulation is given in Figure 7. The H-atoms were formed by the fast reaction of H_2 with the Cl-atoms, which were primarily abstracted from $SiCl_4$. The H-atom profiles closely followed the decomposition of $SiCl_4$. All the rate coefficients k_{17} obtained for the initiation step of $SiCl_4$ thermal decomposition by this procedure are summarized in the Arrhenius diagram of Figure 8. A sensitivity analysis shows that, beside the initiation step and the formation of H-atoms from the $Cl + H_2$ reaction, only the reactions of $SiCl_4$ with H-atoms contribute to the H profiles. It was investigated earlier (Catoire et al., 1996a).

The experiments on $SiCl_4/Ar$ mixtures revealed that absorption of the 121.6-nm radiation by $SiCl_4$ is relatively strong. Thus it was possible to measure the rate of change of

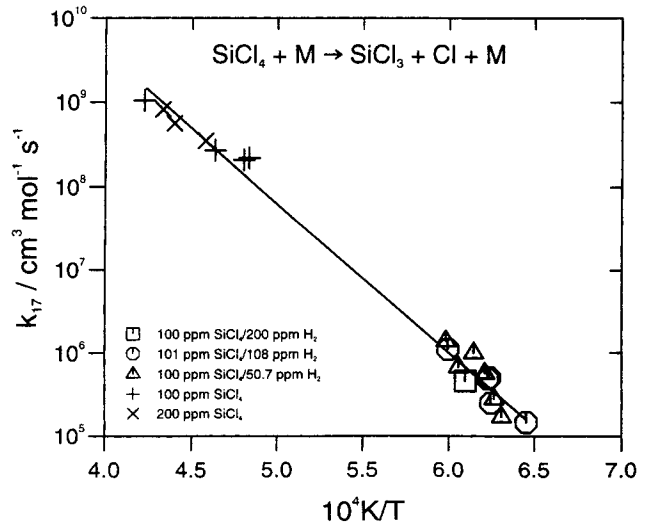

Figure 8. Arrhenius plot for the rate coefficient k_{17}.

the $SiCl_4$ concentration and to obtain additional values for the rate coefficient k_{17} at higher temperatures. They are also given in the Arrhenius diagram of Figure 8. The result of both groups of experiments can be summarized by the following Arrhenius expression:

$$k_{17} = 4.8 \times 10^{16} \exp(-40{,}954\ \mathrm{K}/T)\ \mathrm{cm^3 \cdot mol^{-1} \cdot s^{-1}}.$$

The experimental activation energy represents 73% of the reaction enthalpy.

Further experiments on the pyrolysis of $SiCl_4$ were performed by using ARAS for detecting Si and Cl atoms in experiments at higher temperatures. Si-atoms were monitored in mixtures of 3 to 7 ppm $SiCl_4$ at temperatures between 3,300 K and 3,970 K at pressures between 0.6 and 2.4 bar. A typical Si-concentration profile, showing a plateau after about 150 μs, is shown in Figure 9. A few Cl-atom experiments were also performed at temperatures $3{,}520\ \mathrm{K} \le T \le 3{,}720\ \mathrm{K}$ and pressures between 0.5 and 1 bar in mixtures of 80 and 100 ppm $SiCl_4$ diluted in Ar. At these conditions, $SiCl_4$ decomposes fast into its atomic products and does not interfere with the absorption of Cl atoms. The example data of Figure 10 shows that a Cl-concentration plateau is reached very rapidly.

The interpretation of the Si and Cl experiments was also performed based the reaction mechanism of Table 3. The rate coefficient of reaction R17, determined between 1,550 and 2,370 K, was linearly extrapolated. For reactions R18 and R19, Cl formation was assumed instead of Cl_2 elimination, since the enthalpies of reactions are significantly higher for the elimination process than for the Si–Cl bond-breaking process. Rate coefficients k_{18}, k_{19}, and k_{20} were determined from computer fittings of all measured Si- and Cl-atom profiles. The good agreement between experiments and computations is shown in Figure 9 for the Si-atom experiments and in Figure 10 for the Cl-atom experiments. The mean values of the

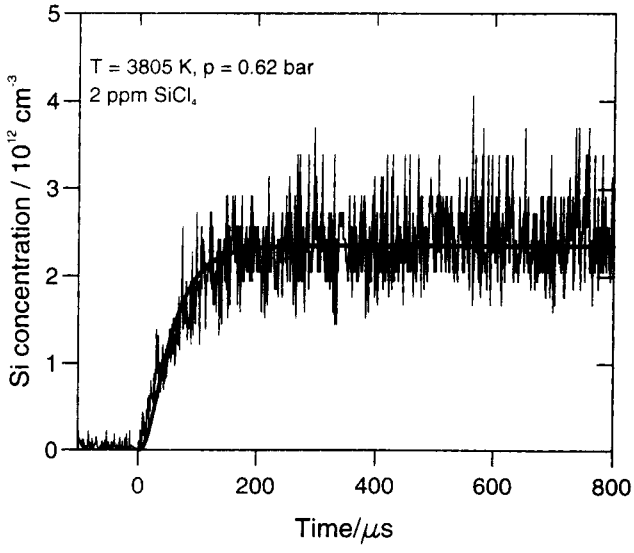

Figure 9. Typical example of measured Si-atom concentration observed in an $SiCl_4$/Ar pyrolysis experiment and comparison with calculated profile.

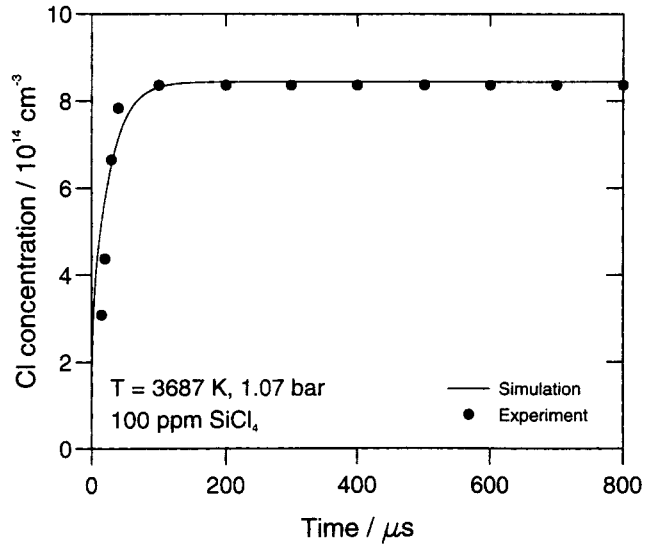

Figure 10. Measured (points) vs. calculated (line) Cl atoms concentration profiles in $SiCl_4$/Ar mixture.

Simulation is based on the reaction mechanism of Table 3.

rate coefficients used can be expressed by the following Arrhenius expressions, which are the results of least-square fits:

$$k_{18} = 3.7 \times 10^{14} \exp(-31{,}730\ \mathrm{K}/T)\ \mathrm{cm^3 \cdot mol^{-1} \cdot s^{-1}}$$

$$k_{19} = 9.4 \times 10^{14} \exp(-43{,}250\ \mathrm{K}/T)\ \mathrm{cm^3 \cdot mol^{-1} \cdot s^{-1}}$$

$$k_{20} = 9.3 \times 10^{14} \exp(-39{,}190\ \mathrm{K}/T)\ \mathrm{cm^3 \cdot mol^{-1} \cdot s^{-1}}.$$

The experimental activation energies represent 97%, 80% and 79% of the reaction enthalpies for the respective reactions.

Photolysis of Silane

The photolysis of silane was studied in gas mixtures of 10 to 50 ppm SiH_4 in Ar in the temperature range between $T =$ 1,040 K and $T = 1{,}210$ K at pressures around 1.1 bar. The excimer laser was fired with a time delay of 50 to 300 μs after the gas was heated by the reflected shock wave. Example data of the SiH_4 photolysis experiment is given in Figure 11. Time zero is fixed to the laser pulse, which, in this example, is approximately 30 μs after the arrival of the reflected shock wave. The formation of Si atoms is very fast, but the peak maximum is reached only with a small delay after the laser pulse, indicating an indirect mechanism for the Si formation. After reaching the maximum, the signal shows a decay during a time period of approximately 75 μs to an almost zero level. This general behavior was found for all SiH_4 photolysis experiments with differences in the peak maxima and in the decay times. A comparison of measured Si concentrations from three photolysis experiments performed at different temperatures is given in Figure 12. With increasing temperature both the yield of Si and the decay time after the peak increase significantly. The maximum Si-yield $[Si]_{max}/[SiH_4]$ obtained from the present photolysis experiments is summarized in Figure 13. The values are between 0.02 and 2.0% and show Arrhenius behavior.

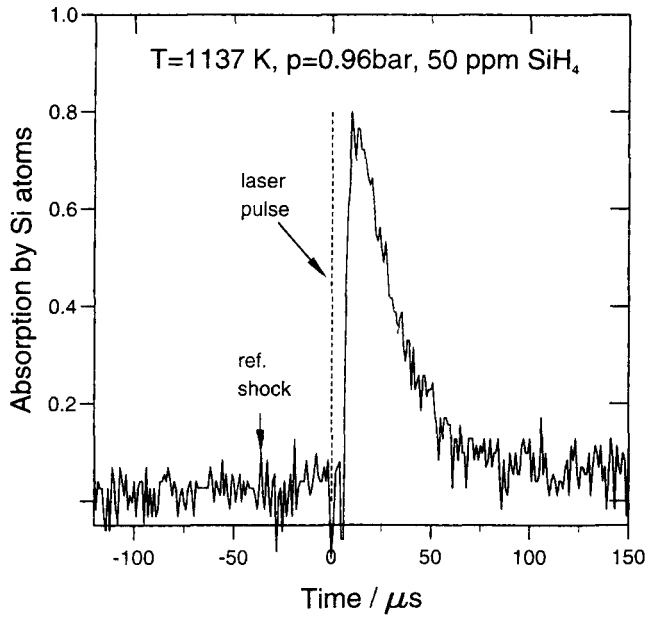

Figure 11. Typical absorption profile of Si-atoms observed in an LFP experiment behind a reflected shock wave.

The Si-atom concentration profiles could be simulated by assuming the energetically possible photodissociation of SiH_4 followed by further reactions of Si, H, SiH, and SiH_4:

$$SiH_4 \xrightarrow{h\upsilon} SiH + H + H_2 \qquad \Delta h^R = 568 \text{ kJ/mol} \qquad \text{(P1)}$$

$$SiH + H \overset{k_{-13}}{\rightleftharpoons} Si + H_2 \qquad \Delta h^R = -144 \text{ kJ/mol} \qquad \text{(R-13)}$$

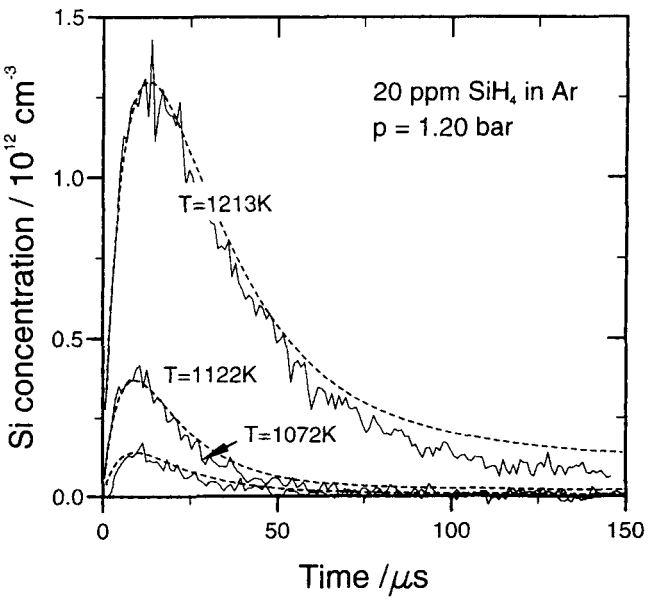

Figure 12. Typical Si concentration measured in LFP experiments at three different temperatures in a mixture with 20 ppm SiH_4 in Ar and comparison with calculated profiles from the reaction mechanism in Table 2.

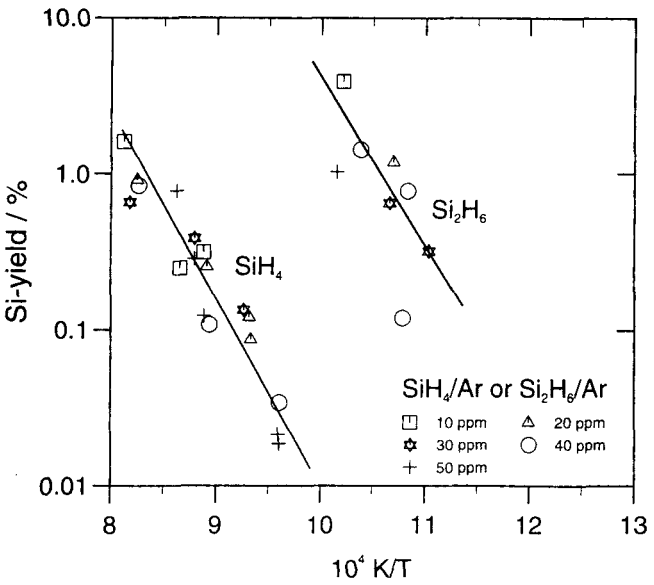

Figure 13. Arrhenius diagram of Si-atom yield measured in LFP experiments of silane and disilane behind reflected shock waves.

$$Si + SiH_4 \overset{k_{14}}{\rightleftharpoons} Si_2H_2 + H_2 \qquad \Delta h^R = -82 \text{ kJ/mol.} \qquad \text{(R14)}$$

Reaction R-13 dominates the formation and reaction R14 the consumption of Si. As the rate coefficient of reaction R13 is relatively well known from direct Si and SiH measurements (see Mick et al., 1995b), the rate coefficient of the Si-consuming reaction R14 could be determined from computer simulations of the measurements using the mechanism of Table 2. Examples of computed Si profiles in comparison with experiments are given in Figure 12. The individual rate coefficient for reaction R14 summarized in the Arrhenius diagram of Figure 14 can be expressed by a temperature-independent value of

$$k_{14} = 4.0 \times 10^{14} \text{ cm}^3 \cdot \text{mol}^{-1} \cdot \text{s}^{-1}.$$

The observed strong temperature dependence of the Si yield in Figure 13 seems to reflect the temperature dependence of both the photolysis reaction P1 and the rate coefficient of reaction R-13.

Photolysis of disilane

The photolysis of disilane was studied in experiments similar to those of silane. The gas mixtures containing 10 to 50 ppm Si_2H_6 diluted in Ar were shock heated to temperatures between $T = 900$ K and $T = 1{,}100$ K at pressures around 1.1 bar. The observed Si absorption profiles appear similar to those of the silane photolysis. The Si-yield for disilane defined by $[Si]_{max}/(2\times[Si_2H_6])$ was found to be between 0.06 and 2%. The individual values obtained are also given in the Arrhenius diagram of Figure 14. The Si-yield also shows Arrhenius behavior, but the values are higher than those found with silane.

For the interpretation of the disilane photolysis experiments, its thermal decomposition into SiH_4 and SiH_2 during

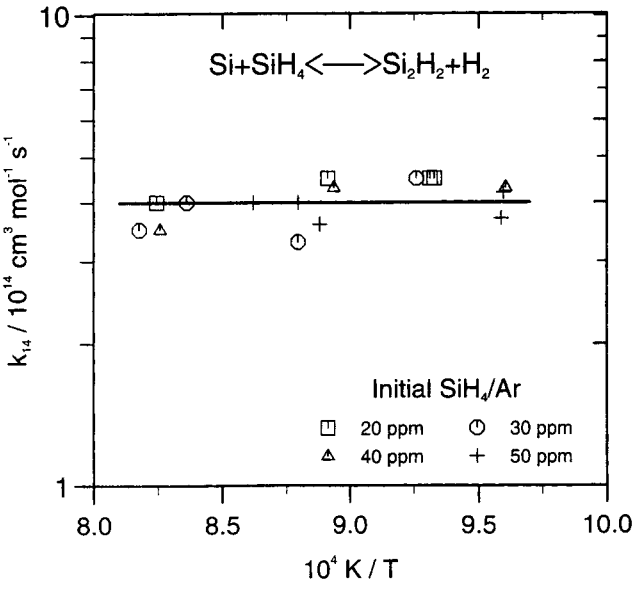

Figure 14. Arrhenius diagram of the rate coefficient k_{14} determined from SiH_4 photolysis and computer simulations with the reaction mechanism in Table 2.

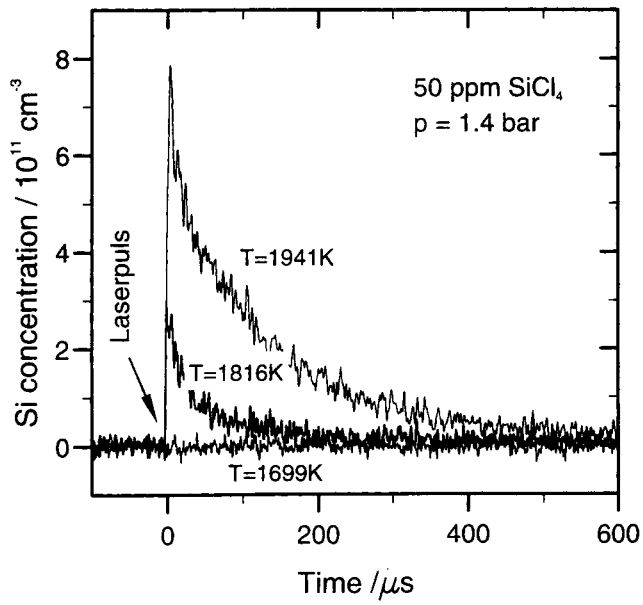

Figure 15. Typical Si concentration measured in LPF experiments in a mixture with 50 ppm $SiCl_4$ in Ar.

the time interval between reflected shock and laser pulse must be included, that is, the initial composition for the photolysis differs from the initial gas composition. This was calculated using the mechanism of Table 2. The further Si concentration profiles after the laser pulse could be simulated by regarding the energetically favorable photolysis of Si_2H_6

$$Si_2H_6 \xrightarrow{h\upsilon} SiH_4 + SiH + H \qquad \Delta h^R = 554\ \text{kJ/mol} \quad \text{(P2)}$$

as the initiating step. The kinetically delayed Si-atom formation is, as in the case of silane, controlled by the reaction R-13, and is followed by the strongly dominating Si-consuming reaction R15

$$Si + Si_2H_6 \overset{k_{15}}{\rightleftharpoons} Si_3H_2 + 2H_2 \qquad \Delta h^R = -148\ \text{kJ/mol} \quad \text{(R15)}$$

with a small contribution of reaction R14. Using the known rate coefficients k_{13} and k_{14}, the measured Si-concentrations could be fitted by varying rate coefficient k_{15}. Over the temperature range between $T = 900$ K and $T = 1{,}100$ K we found:

$$k_{15} = 4.8 \times 10^{14}\ \text{cm}^3 \cdot \text{mol}^{-1} \cdot \text{s}^{-1}.$$

Photolysis of silane tetrachloride

The photolysis of silane tetrachloride was studied by Si-atom measurements in gas mixtures of 50 ppm $SiCl_4$ in the temperature range between $T = 1{,}700$ K and $T = 1{,}940$ K at pressures around 1.4 bar. Example data for three different temperatures are shown in Figure 15. A strong temperature dependence of the Si-formation is again obvious. At temperatures below 1,700 K the Si-concentration remains below the detection limit. With increasing temperature the Si-yield $[Si]_{max}/[SiCl_4]$ increases up to 0.3%. At temperatures above $T = 2{,}000$ K the thermal decomposition of $SiCl_4$ must also be taken into account. The decay of Si in all $SiCl_4$ photolysis experiments is slower than it was for comparable SiH_4 experiments.

Bimolecular Si-atom reactions

Bimolecular Si-atom reactions were studied using the fast pyrolysis of silane as a Si-atom source. The general kinetic methodology can be illustrated in the example reaction of Si atoms with CO:

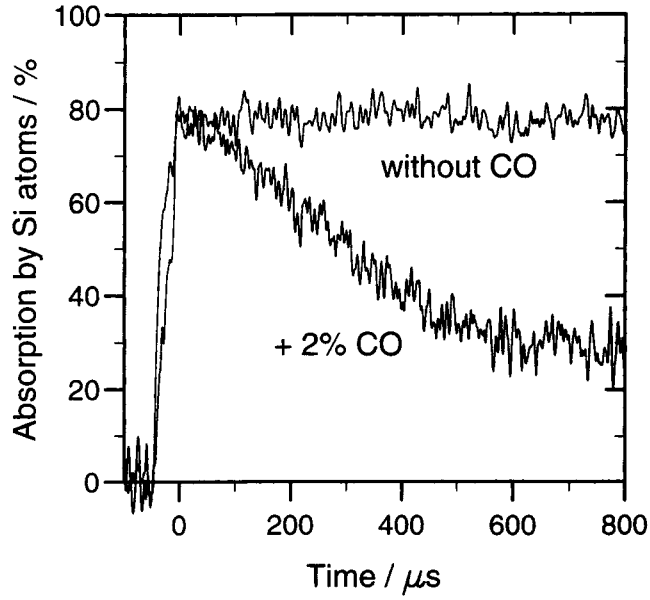

Figure 16. Typical Si absorption measured in pyrolysis experiments with 1 ppm SiH_4 without and with CO addition.

Table 4. Rate Coefficients of Various Si-Atom Reactions Obtained by ARAS*

	Reaction			A_i	C_i
R26	$Si+CO$	$\rightarrow$	$SiO+C$	7.8×10^{14}	34,510
R27	$Si+CO_2$	$\rightarrow$	$SiO+CO$	6.0×10^{14}	9,420
R28	$Si+NO$	$\rightarrow$	$SiO+N$	3.2×10^{13}	1,775
R29	$Si+O_2$	$\rightarrow$	products	2.7×10^{14}	1,765
R30	$Si+N_2O$	$\rightarrow$	$SiN+NO$	5.0×10^{14}	8,100
		$\rightarrow$	$SiO+N_2$	8.0×10^{13}	0

*$k_i = A_i \exp(-C_i/T)$ $cm^3 \cdot mol^{-1} \cdot s^{-1}$.

$$Si + CO \xrightarrow{k_{26}} SiO + C \qquad \Delta^R h = 276 \text{ kJ/mol.} \qquad \text{(R26)}$$

This reaction was studied in mixtures containing 0.75 to 20 ppm SiH_4 and 0.2 to 5% CO diluted in Ar at temperatures 2,720 K $\leq T \leq$ 5,190 K using the Si atom ARAS as given in Figure 1. Example profiles of Si absorption measured in mixtures without and with CO are given in Figure 16. Immediately behind the reflected shock wave, the precursor SiH_4 decomposes nearly instantaneously to form Si atoms (and H_2) at a constant level. In the presence of CO, the silicon atoms are removed by reaction R26, resulting in a decrease in the Si absorption. As CO is in high excess, the kinetic evaluation of the disappearance of Si can be made assuming first-order conditions.

$$d\ln[Si]/dt = -k_{26}[CO]_0. \qquad (4)$$

The Si-concentration in Eq. 4 can be substituted by the measured absorption using the Lambert-Beer law of Eq. 1, and the rate coefficient k_{26} can be evaluated directly from the observed decay of the absorption signal. The Arrhenius expression for the rate coefficient k_{26} is given in Table 4, which also contains a summary of the other bimolecular Si-atom reactions, and the respective rate coefficients are determined. For more details, see Mick et al. (1993b), and Mick and Roth (1994a,b).

Acknowledgments

The financial support of the Deutsche Forschungsgemeinschaft (DFG) and of the Ministerium für Wissenschaft und Forschung des Landes Nordrhein-Westfalen (MWF-NRW) is gratefully acknowledged. One of the authors (L.C.) thanks DRETDGA for financial support. The authors also thank Dr. H. J. Mick and Dr. M. W. Markus for their contribution to the SiH_4 and Si_2H_6 pyrolysis study in the framework of their PhD theses. We further thank Mrs. C. Kmiecik, Mrs. N. Schlösser, and Mr. A. Kunz for their help in conducting the experiments.

Literature Cited

Breiland, W. G., P. Ho, and M. E. Coltrin, "Gas-Phase Silicon Atoms in Silane Chemical Vapor Deposition: Laser-Excited Fluorescence Measurements and Comparisons with Model Predictions," *J. Appl. Phys.*, **60,** 1505 (1986).

Catoire, L., D. Woiki, and P. Roth, "A Shock Tube Study of the Reaction of H Atoms with $SiCl_4$," *Int. J. Chem. Kinet.*, **29**, 469 (1997a).

Catoire, L., D. Woiki, and P. Roth, "Kinetics of the Initiation Step of the Thermal Decomposition of $SiCl_4$," *Int. J. Chem. Kinet.*, **29**, 475 (1997b).

Coltrin, M. E., R. J. Kee, and J. A. Miller, "A Mathematical Model of Silicon Chemical Vapor Deposition," *J. Electrochem. Soc.*, **133,** 1206 (1986).

Markus, M. W., and P. Roth, "A Quantitative Ring Dye Laser Absorption Diagnostic for Free SiH_2 (X^1A_1) Radicals at High Temperatures," *J. Quant. Spectrosc. Radiant. Transf.*, **52,** 783 (1994).

Markus, M. W., and P. Roth, "Development of a Quantitative Ring Dye Laser Absorption Diagnostic for a Free SiH Radicals," *J. Quantum Spectrosc. Radiant. Transf.*, **56**, 489 (1996).

Mick, H. J., V. N. Smirnov, and P. Roth, "ARAS Measurements on the Thermal Decomposition of Silane," *Ber. Bunsenges. Phys. Chem.*, **97,** 793 (1993a).

Mick, H. J., H. Matsui, and P. Roth, "High Temperature Kinetics of Si Atom Oxidation by NO Based on Si, N, and O Atom Measurements," *J. Phys. Chem.*, **97,** 6839 (1993b).

Mick, H. J., and P. Roth, "High Temperature Kinetics of $Si+N_2O$," *J. Phys. Chem.*, **98,** 5310 (1994a).

Mick, H. J., and P. Roth, "Shock Tube Study of Silicon Atom Oxidation by CO and CO_2," *J. Phys. Chem.*, **98,** 7844 (1994b).

Mick, H. J., M. W. Markus, P. Roth, and V. N. Smirnov, "A Shock Tube Study of the Thermal Decomposition of Si_2H_6 Based on Si and SiH_2 Measurements," *Ber. Bunsenges. Phys. Chem.*, **99,** 880 (1995a).

Mick, H. J., T. Kruse, and P. Roth, "A Shock Tube Study of the Reaction $Si + H_2 \rightarrow SiH + H$," *Proc. Int. Symp. Shock Waves ISSW20,* World Scientific Publishing, NJ, p. 875 (1996).

Thielen, K., and P. Roth, "Resonance Absorption Measurements of N, O, and H Atoms in Shock Heated $HCN/O_2/Ar$ Mixtures," *Combust. Flame*, **69,** 141 (1987).

Woiki, D., M. W. Markus, and P. Roth, "A Shock Tube-Laser Flash Photolysis Study of the Reaction $COS+S \rightleftharpoons CO+S_2$," *J. Phys. Chem.*, **97,** 9682 (1993).

Woiki, D., and P. Roth, "A Shock Tube Study on the Thermal Decomposition of CS_2 Based on $S(^3P)$ and $S(^1D)$ Concentration Measurements," *Shock Wave*, **4**, 95 (1994).

Manuscript received Oct. 28, 1996, and revision received Apr. 2, 1997.